High Energy Physics and Nuclear Physics

Volume 16, Number 3

Measurement of Complete Fusion Excitation Function of $^{16}O + ^{28}Si$ Reaction

Zheng Jiwen[1], Zheng Pingzi[1], Liu Guoxing[1], Chen Keliang[1], Wang Sufang[1], Bai Xingping[1] and Yu Xian[1], Zhang Huanqiao[2], Xu Jincheng[2], Liu Zuhua[2], Ruan Ming[2], Lü Jun[2] and Xu Kan[2]

[1]Institute of Modern Physics, the Chinese Academy Sciences, Lanzhou, Gansu, China
[2]Institute of Atomic Energy, Beijing, China

The complete fusion excitation function of the $^{16}O + ^{28}Si$ reaction is measured in the 50-90 MeV range with 1.0 MeV in step. By using some theoretical models, the result is analyzed and model parameters extracted. The gross structure is found in the excitation function when $E_{CM} < 46$ MeV. The energies of peaks are 34.5, 38.5 and 43.0 MeV, respectively. The structure vanishes gradually when $E_{CM} > 46.0$ MeV.

1. INTRODUCTION

So far there are abundant data of complete fusion excitation functions in the low energy region (< 10 MeV/A), which reveals the change of the restriction mechanism of the complete fusion reaction with the bombarding energy. Experiments showed that a very important phenomenon, the energy-dependent resonant-like structures, appear in the fusion excitation functions of some light systems. These structures overlay on the smooth curves described by the potential barrier model. The nearly periodic oscillations with several MeV in width were first observed in the fusion excitation functions of the $^{12}C + ^{12}C$, $^{12}C + ^{16}O$ and $^{16}O + ^{16}O$ reactions [1]. This type of oscillation is called the gross structure. Afterwards the gross structures were also observed in the $^{12}C + ^{24}Mg$, ^{28}Si and ^{18}O and $^{14}C + ^{16}O$ systems. The intermediate structures with several hundred keV in width were observed in the $^{12}C + ^{16}O$, ^{28}Si and ^{32}S and $^{16}O + ^{20}Ne$ system.

Supported by the Science Foundation of the Chinese Academy of Sciences.
Received on January 7, 1991.

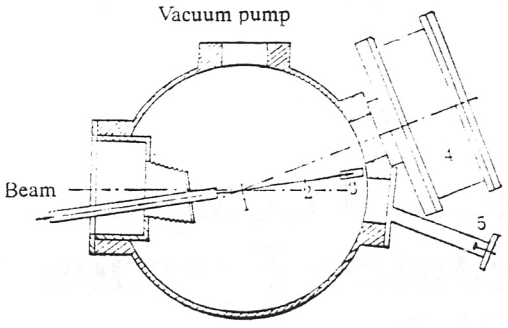

Fig. 1
Schematic diagram of the experimental set-up.
1. Target; 2. Gold target; 3. Faraday cup;
4. ΔE-E telescope system; 5. Monitor.

It is noteworthy that for all systems composed by ^{12}C and α-cluster nuclei, such as ^{12}C + ^{12}C, ^{16}O, ^{20}Ne, ^{24}Mg, ^{28}Si and ^{32}S, etc., the complete fusion excitation functions have distinct structures. Thus, it is very interesting to know whether the complete fusion excitation functions have structures in the systems composed by ^{16}O and α-cluster nuclei, for example, ^{16}O + ^{12}C, ..., and ^{40}Ca. Except for the above-mentioned ^{16}O + ^{12}C, ^{16}O and ^{20}Ne systems, one also observed the structure in the ^{16}O + ^{40}Ca system. However, no one has observed structures in the ^{16}O + ^{24}Mg, ^{28}Si and ^{32}S systems so far. Thus, it is necessary to study these systems further. Rascher *et al.* [2] reported that they had not observed the distinct structure in the ^{16}O + ^{28}Si system in the larger energy region in their experiment. Many investigations were conducted about the elastic scattering in this system [3,4], which indicated that two excitation functions at θ_{CM} = 90° and θ_{CM} = 180°, respectively, have gross structures and anti-correlation in the overlapping energy region. Because both the enhancement of the backward-angle elastic scattering cross-section and the structure of the fusion excitation function originate from the nuclear molecule phenomenon, the complete fusion excitation function of the ^{16}O + ^{28}Si reaction may have the structure. Therefore, we measured the complete fusion excitation function in the 50-90 MeV range with 1.0 MeV in step for this system.

2. EXPERIMENTAL PROCEDURE

The experiment was carried out at the 2 × 13 MeV tandem accelerator in the Institute of Atomic Energy, Beijing. The ^{16}O beam was generated by the accelerator, and guided into a scattering chamber with 38 cm in diameter from an aperture with 16 cm in diameter located in the front of the chamber. The scattering chamber can be rotated ±10° around its vertical axis in the reaction plane, with the beam tube fixed. Two apertures of 7 cm in diameter are located at the terminals of the scattering chamber, which stretch an angle of 18° with respect to the center of the chamber. The ΔE-E telescope system used to measure evaporation residues is connected with one of the apertures. A solid state detector used to measure scattering particles is installed onto another aperture. The target is placed in the center of the scattering chamber and is perpendicular to the beam direction. In order to measure Coulomb scattering particles, a 100 μg/cm^2-thick gold target is placed at the place 9.5 cm behind the center of the chamber. The Faraday cup placed behind the gold target is used to measure the beam intensity. The experimental set-up is shown in Fig. 1.

The entrance window of the ΔE-E telescope system is 30 cm away from the target. The distance between the centers of two neighboring entrance windows is 1.25 cm and the spanned angle is 2.4°. The window aperture of the scattering chamber with a stretching angle of 18° can cover 8 entrance windows of the detector; consequently, the range of the measurement angle is 22°-39°, when the

scattering chamber rotates to the left limit. The transmission-type ΔE detector of the ΔE-E telescope system is a flow-up ionization chamber. Its entrance window consists of 10 small linearly arranged apertures with 1.0 cm in diameter. The gas filling the ionization chamber is a steady flow of 90% argon and 10% metrance. The effective gas space length is 6 cm. The gas pressure is about 2660 Pa, and its long-term stability is better than 3%. The E detector consists of 10 gold surface barrier silicon detectors with an effective diameter of 8 mm. They aim at 10 small apertures, respectively. Thus, we set up a position-sensitive ΔE-E telescope with 10 different measurement angles. In terms of a multi-parameter data collect system, we obtained the ΔE-E two-dimensional spectra and recorded them on the magnetic tape.

In order to decrease the relative error of the cross-section, we tried our best to keep all measurement conditions unchanged throughout the experiment. For each bombarding energy, we collected the data in the 5°-22° range, which covers the main angular distribution region of the high cross section. In order to obtain cross-sections at large angles and constitute the complete angular distribution, we also measured fusion cross sections in the 22°-44° range at E_L = 55, 70 and 85 MeV.

3. EXPERIMENTAL RESULTS AND DISCUSSION

The angular distributions of evaporation residues were measured in the θ_L = 5°-40° range at E_L = 55, 70 and 85 MeV. According to the statistical evaporation theory of the compound nuclei, if the particle evaporation of the compound nuclei is isotropic in the center of mass system, the angular distribution of the residue in the laboratory system can be written as

$$\frac{d\sigma}{d\Omega} = N\cos^2\theta_L \exp\left[-V_c^2\sin^2\theta_L/2\sigma_\theta^2\right], \tag{1}$$

where V_c is the recoil velocity of the compound nuclei, which is the center of mass velocity in the complete fusion reaction, N is the normalization constant, and the distribution width parameter σ_θ reflects the recoil velocity of the residue caused by the particle evaporation in the center of mass system. We found that Eq.(1) is feasible only in the finite angular range (< 15°) in fitting our angular distributions. The values of σ_θ^2 obtained from the θ_L < 15° experimental points were 0.00931, 0.0141 and 0.0189 cm^2/ns^2, respectively, and had a linear relationship with the excitation energy of the compound nuclei. This is consistent qualitatively with that predicted according to the evaporation theory. The experimental values of angular distributions at θ_L > 15° were all larger than those obtained from fitting data in the small angular region by Eq.(1). It shows that many contributions are given by the component of the α-particle evaporation at large angles. In the measurement of the excitation function, we only collected the data in the 5°-22° range.

To calculate the total cross-section by integrating the angular distribution over all angles, we had to take the cross-section values at θ_L < 5° by using Eq.(1) which fits the experimental curve, because no experimental points exist in this angular region. The contribution from this part of cross-sections to the total cross-section decreased with the increasing bombarding energy. They are 21.4%, 18.8% and 16.3% at E_L = 55, 70 and 85 MeV, respectively. The contributions from cross-sections in the θ_L > 22° range were 3.4%, 4.6% and 6.2% at above mentioned energies, respectively. In other words, this part of contribution increased with the increasing bombarding energy and was, in general, very small. By extrapolating and interpolating experimental values, we can estimate this part of contribution at the other bombarding energy. Because of the thickness of the target and finite thicknesses of the entrance window and filled gas space, the residue nuclei below a certain energy could not reach the E detector and stopped in the ΔE detector. Thus, the telescope system has a threshold value Q. The influence of this effect decreased with the increasing bombarding energy. We can estimate that this part of loss may reach to 10% at E_L = 50 MeV, and decrease to 2% at E_L = 90 MeV. By assuming that this loss depends linearly on the bombarding energy, we can correct the cross-section.

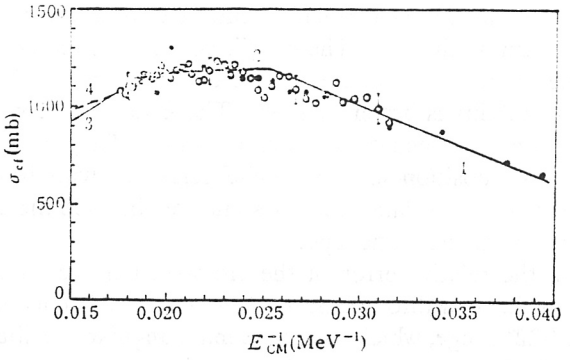

Fig. 2
The complete fusion excitation function for the $^{16}O + ^{28}Si$ reaction.
1. Barrier transmission model; 2. Critical distance or statistical yrast line model; 3. Saturation angular momentum; 4. Fusion entry line.

In the error calculation for the complete fusion cross-section, we took into account the statistical error, the error of the target thickness, the error of division residues, the correction error of the low energy loss in detectors, the error of the detector angle in using the normalization of the Coulomb scattering cross-section, and the error of the current integration in normalizing the cross-section in terms of the total count of ions. We also estimated the correction error in the large and small angular regions in calculating the total cross-section by using the integration of the angular distribution. The error bar of the total fusion cross-section was about 8.0% in the low energy region and 6.2% in the high energy region.

We plotted the complete fusion excitation function of the $^{16}O + ^{28}Si$ reaction in Fig. 1. This figure shows the change of the fusion cross-section with the variation of the incident energy in the E_{CM} = 31.8-57.3 MeV range. When the bombarding energy increased, the fusion cross-section increased at E_{CM} < 43 MeV, hardly changed at E_{CM} = 43-53 MeV and probably had the decreasing trend at E_{CM} > 53 MeV. We also plotted the experimental results obtained by Rascher *et al.* in Fig. 1. Except for very large deviations at two highest energy points in the E_{CM} = 22-51 MeV range, their results are in agreement with ours in the E_{CM} = 31.8-46 MeV range.

In the low energy heavy ion reaction, one can describe the complete fusion excitation function by using the potential barrier model. Based on this model, the fusion occurs only if the projectile can penetrate the interaction barrier of two nuclei. If one ignores the quantum effect, the relationship between the cross-section and energy can be written as

$$\sigma_{cf} = \pi R_B^2 \left(1 - \frac{V_B}{E}\right), \tag{2}$$

where V_B and R_B are the fusion barrier and barrier radius, respectively. When the incident energy becomes higher, whether the barrier can be penetrated is no longer the condition of the complete fusion. Instead, whether the minimum approaching distance between two interaction nuclei can reach the critical distance R_{cr} becomes the fusion condition [5]. Then, we write the fusion cross-section as

$$\sigma_{cf}(E) = \pi R_{cr}^2 \left(1 - \frac{V_{cr}}{E}\right), \tag{3}$$

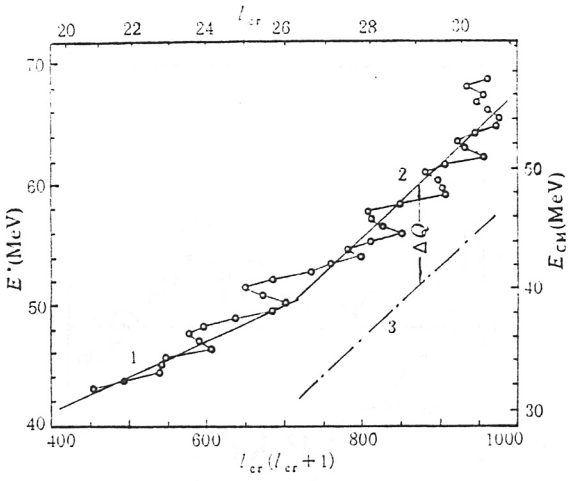

Fig. 3
The critical angular momentum for the $^{16}O + {}^{28}Si$ fusion reaction.
1. Barrier line; 2. Critical distance line; 3. Yrast line.

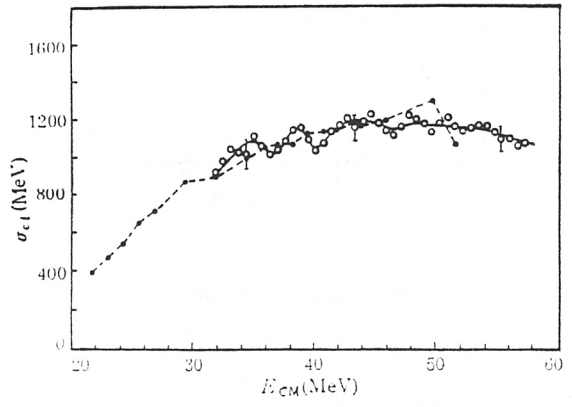

Fig. 4
The complete fusion excitation function for the $^{16}O + {}^{28}Si$ reaction.
○ Present work; ● R. Rascher *et al.*

where R_{cr} is the critical distance and V_{cr} is the interaction potential at the critical distance. The model parameters extracted from the data of the present work and Rascher's by using Eqs.(2) and (3) are as follows: R_B = 8.33 fm (r_B = 1.55 fm), V_B = 17.9 MeV, R_{cr} = 5.88 fm (r_{cr} = 1.06 fm) and V_{cr} = —3.0 MeV. These values are consistent with the systematic values. In this energy region, another explanation is that the properties of the compound nucleus restricts the process of the complete fusion. Lee *et al.* [6] proposed that the statistical yrast line parallel to the yrast line in a distance of ΔQ restricts the process of the complete fusion. At this time, the compound nucleus possesses a certain amount of internal excitation energy ΔQ, hence a rather high level density. Thus, the complete fusion can occur. According to this model, the fusion cross-section can be written as

$$\sigma_{cf}(E) = \frac{\pi \mathscr{T}_0}{\mu}\left[1 + \frac{Q - \Delta Q}{E}\right], \tag{4}$$

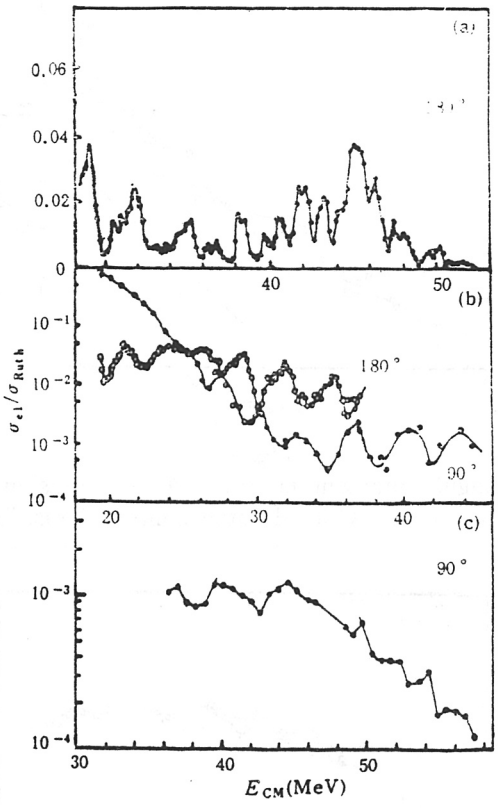

Fig. 5
The excitation function of the elastic scattering for the $^{16}O + ^{28}Si$ reaction.
(a) P. Brauu-Munzinger *et al.* [4]; (b) S. Kubono *et al.* [8]; (c) Present work.

where $\mathscr{T}_0$ is the moment of inertia of the compound nucleus, μ is the reduced mass, and Q takes the ground state Q value of the fusion reaction. By using the rigid moment of inertia, the experimental data for light systems ($A_1 + A_2 < 80$) is analyzed, and the radius parameter of the compound nucleus obtained as $r_0 = 1.20 \pm 0.05$ fm. The distance from the statistical yrast line to the yrast line is 10 ± 2.5 MeV. The parameters obtained by using Eq.(4) to fit our data are: $r_0 = 1.26$ fm, $\Delta Q = 8.3$ MeV. They are also in the reasonable range. Therefore, from the fusion excitation function of the $^{16}O + ^{28}Si$ reaction, we cannot distinguish whether the critical distance of the entrance channel or the statistical yrast line restricts the fusion reaction.

The critical angular momentum as a function of the energy is plotted in Fig. 3. l_{cr} is calculated from the measured fusion cross-section,

$$\sigma_{cf} = \pi\lambda^2(l_{cr} + 1)^2 \tag{5}$$

Fig. 3 shows that when $E > 53$ MeV, l_{cr} varies between 30 and 31 and is in the saturation status. Curve 3 in Fig. 2 corresponds to the fusion cross-section where the critical angular momentum is taken to be the saturation value 30.4. The fusion entry line proposed by Matsuse *et al.* [7] may also be the restriction mechanism of the fusion reaction in this energy region. According to this model, the fusion condition of two colliding nuclei is that the minimum approaching distance must be a value

less than $<d^2>^{\frac{1}{2}}$, where $<d^2>^{\frac{1}{2}}$ is the root mean square distance between nuclei A_1 and A_2, which is given by

$$\frac{A_1 A_2}{A}\langle d^2\rangle = A\langle r^2\rangle_A - A_1\langle r^2\rangle_{A1} - A_2\langle r^2\rangle_{A2}, \tag{6}$$

where A_1, A_2 and A are the mass numbers of the projectile and target nuclei and compound nucleus, respectively. In the $^{16}O + ^{28}Si$ reaction, $<d^2> = 13.94$ fm^2. Straight line 4 in Fig. 2 denotes the fusion cross-section calculated in this model. Fig. 2 also shows that when $E_{CM} > 50$ MeV, all experimental points are located above this restriction line. Thus, the fusion entry line does not give a distinct restriction to the complete fusion reaction in this system.

There is one difference between our fusion excitation function and Rascher's. Rascher's fusion excitation function varies smoothly with the change of the bombarding energy. Except for two highest energy points, it does not have so much fluctuation. However, our excitation function is not a smoothly varying function. The cross-section with respect to the incident energy has a larger and regular fluctuation. When $E_{CM} < 46$ MeV, it exhibits the gross structure. The peaks of oscillations appear mainly at $E_{CM} = 34.5$, 38.5 and 43.0 MeV (see Fig. 4). When $E_{CM} > 46$ MeV, the fluctuation of experimental points are within the error bar, therefore we cannot confirm the existence of the structure. In general, the structures of the excitation functions of the fusion and elastic scattering at a particular angle may originate from the same mechanism, thus these two structures may have some correlations. The elastic scattering excitation functions measured at 180° for the $^{16}O + ^{28}Si$ reaction by Barrette *et al.* [3] and Braun-Munzinger *et al.* [4] are shown in Fig. 5. The excitation functions of the elastic scattering at 90° and 180° measured by Kubono *et al.* are also given in this figure. As shown in Fig. 5(b), the gross structures of two excitation functions are anti-correlated. The peak position of the elastic scattering excitation function measured by Kubono *et al.* at 180° corresponds to 35 MeV in our experiment. The peaks given by Braun-Munzinger *et al.* are at 35, 38.5, 42, 45 and 47.5 MeV, respectively, and generally agree with our results. According to the experimental error, our excitation function in the 41-46 MeV range can only be considered a unique convex. It is also difficult to confirm the existence of the peak around 47.5 MeV. Thus, we measure the excitation function of the elastic scattering at 90° with a larger angular spread (±5°) (see Fig. 5(c)). The mean cross-section hardly changes with the variation of the incident energy when $E_{CM} < 46$ MeV. It resembles the result given by Kubono *et al.* The fact that the larger oscillation like Kubono's is not observed in our experiment is possibly due to the poor angular resolution; but in the $E_{CM} < 46$ MeV region, their gross structures are the same. On the other hand, our excitation function $\sigma_{el}/\sigma_{Ruth}(90°)$ in the $E_{CM} > 46$ MeV region decreases exponentially with the increasing incident energy. This behavior also appears in the excitation function of the elastic scattering at 180° given by Braun-Munzinger *et al.* The fact that the elastic scattering cross-section decreases with the increasing bombarding energy shows that the enhancement of the backward-angle-elastic scattering becomes weaker. It seems that this effect corresponds to the loss of the structure of the fusion excitation function in this energy range.

REFERENCES

[1] P. Sperr *et al.*, *Phys. Rev. Lett.*, **36** (1976) 405; *Phys. Rev. Lett.*, **37** (1976) 321.
[2] R. Rascher *et al.*, *Phys. Rev.*, **C20** (1979) 1028.
[3] J. Barrette *et al.*, *Phys. Rev. Lett.*, **40** (1978) 455.
[4] P. Braun-Munzinger *et al.*, *Phys. Rev.*, **C24** (1981) 1010.
[5] J. Galin *et al.*, *Phys. Rev.*, **C9** (1974) 1018.
[6] S. M. Lee *et al.*, *Phys. Rev. Lett.*, **45** (1980) 165.

[7] T. Matsuse *et al.*, Proceedings of Tsukuba International Symposium on Heavy Ion Fusion Reaction, Tsukuba, 1984.
[8] S. Kubono *et al.*, *Phys. Rev.*, **C21**(1980)495; *Phys. Lett.*, **84B** (1979) 408.